International Journal of Hybrid Information Technology
Vol. 9, No.8 (2016), pp. 409-416
http://dx.doi.org/10.14257/ijhit.2016.9.8.36

A Medical Image Fusion Algorithm based on Non-subsampled Shearlet Transform and Non-negative Matrix Factorization

Chen Zhen[1], Xing Xiaoxue[2], Guo Pan[3] and Fan Qinyin[4]

1. Information Engineering Department, Putian University, Putian, China ,35110
2. College of Information Engineering, Changchun University, Changchun, China, 130022
3. Institute of Science and Technology，College of Humanities & Sciences of Northeast Normal University, Changchun, China, 130022
4. School of Engineering, Osaka University, Osaka, Japan, 5650871
Corresponding Author: CHEN Zhen
chenfjpt@yeah.net

Abstract

After the image decomposition with Non-subsampled Shearlet Transform (NSST), the transform coefficients have a larger redundancy. In order to reduce the redundant information, an image fusion algorithm based on NSST and non-negative matrix factorization (NMF) is introduced. The source images are decomposed with NSST into the low-frequency coefficients and the high-frequency sub-band coefficients. The low-frequency coefficients are fused based on NMF theory. The high-frequency coefficients are fused based on Regional Sum Modified-Laplacian (SML) Maximum. Finally, the inverse NSST is used to reconstruct the final fused image. The proposed algorithm can effectively remove redundant information, extract global features and capture more direction details information of multi-source image. Experiments show that the proposed algorithm has obvious advantages and the fused image quality has been greatly improved. The presented algorithm is superior to other fusion algorithms from the objective parameters.

Keywords: *Image Fusion; NSST; NMF; SML*

1. Introduction

With the development of medical technology, medical images in medical diagnostics are playing an increasingly important role. Multi-modality medical image information obtained from different medical imaging equipment can describe more morphological and functional information of same human organs which can't be acquired in single medical image. In order to provide the more valuable information and more accurate reference to medical diagnosis and cure, the medical images fusion technology is used to integrate the different information which comes from different medical imaging equipment.

The Non-subsampled Shearlet Transform (NSST) is one of the state-of-the-art MGA tools in [1-3], which could realize the truly sparse representation at various directions and different scales of image. NSST could be used to fuse the image to get better fusion effects. When the source images are decomposed with NSST, the transform coefficients have great redundancy. NSST is essentially a redundant transform, which can not be used alone to remove redundant information effectively.

Non-negative matrix factorization (NMF) is a new analysis method proposed in recent years for decomposition of non-negative data. The method is used for statistical analysis of multivariate data, imposes non-negative constraints on coefficients to give linear expression of original data,and was developed by Lee and Seung in [4-5]. NMF is often

ISSN: 1738-9968 IJHIT

used to nonlinearly locate purely additive, parts-based, linear, and sparse representations of the non-negative multivariate data. It can reveal the latent structure, feature and pattern of the input data. After NMF decomposition the matrix elements become non negative. The requirement of non-negative constraints makes many multi-focus image fusion methods based on NMF developed in [6-12].

An image fusion algorithm based on NSST and NMF is introduced in this paper. On the one hand, NSST can fully extract details form multiple directions of the source image. On the other hand, NMF can effectively remove the redundant information. The algorithm can maximize the retention of the edge and feature information of the two images, and greatly reduce the computational complexity, and improve the image visual effects and anti-interference ability.

2. Related Work

2.1. Non-subsampled Shearlet Transform

K.Guo and G.Easley put forward shearlet transform. The shearlet is reconstructed through using affine system with composite dilations. When the dimension x equals 2, the affine system $A_{AB}(\psi)$ with synthesis expansion are expressed in equation (1) in [13-14]. If $A_{AB}(\psi)$ has the form of Parseval frame (also known as tight frame), the elements of the system are called composite wavelets.

$$A_{AB}(\psi)=\{\psi_{j,l,k}(x)=|\det A|^{j/2}\psi(B^l A^j x-k): j,l\in Z,k\in Z^2\} \tag{1}$$

Among them, $\psi\in L^2(R^2)$, $|\det B|=1$, A and B are 2×2 invertible matrices. Shearlets are expressed in equation (2),

$$SH_\psi f(a,s,t)=\langle f,\psi_{a,s,t}\rangle, a>0, s\in R, t\in R^2 \tag{2}$$

$\psi_{a,s,t}$ is defined as follows,

$$\psi_{ast}(x)=|detM_{as}|^{1/2}\psi(M_{as}^{-1}(x\text{-}t)) \tag{3}$$

$$M_{as}=B_sA_a \qquad A_a=\begin{pmatrix} a & 0\\ 0 & \sqrt{a}\end{pmatrix} \qquad B_s=\begin{pmatrix} 1 & s\\ 0 & 1\end{pmatrix} \tag{4}$$

where A_a is an anisotropic dilation matrix, and B_s is a shear matrix.

Figure 1 is a subdivision graph of shearlets in frequency domain, which has the geometric features of subdivision area.

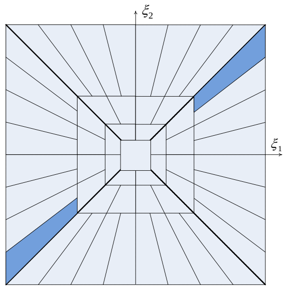

(a) The tiling of the frequency plane

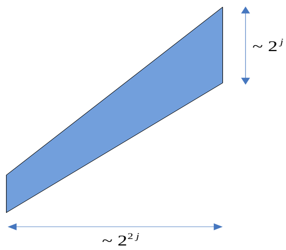

(b) Shearlet frequency supports

Figure 1. Frequency Partition and the Support of One Shearlet

The standard shearlet filter is realized through the translation operation of window function in pseudo polarization lattice. Because the implementation process need to carry out the sampling operation, it does not have the translation invariance. When the image is reconstructed , pseudo Gibbs phenomenon will emerge. So G.Easley and K.Guo *et al*. put forward NSST.

The block diagram of shear wave transformation in the fixed resolution level j is shown in Figure 2. The implementation is mainly divided into two steps: non-subsampled Multi-scale decomposition and the directional localization in [15-16]. Non-subsampled Pyramid (NSP) using the two-channel non-subsampled filter banks makes NSST have a feature of multi-scale. The low frequency coefficient f_a^1 and the high frequency coefficient f_d^1 of image are obtained after a layer of NSP decomposition of the source image. Then each subsequent layer of NSP decomposition iterates the low frequency components obtained from the upper NSP decomposition to get the singular points of the image.

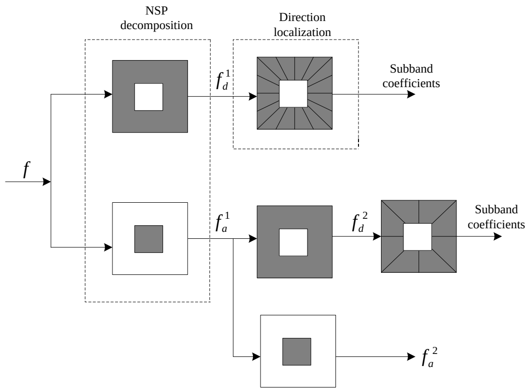

Figure 2. Schematic Two Level Decomposition of NSST

2.2. Theory of Non-negative Matrix Factorization

In 1999 D. D. Lee and H. S. Seung firstly proposed the concept of the non-negative matrix factorization (NM). It is a new method to analyze the non-negative data and can reveal the low dimensional structure of data in high dimensional space. The partial linear expression of the data and base vectors which makes the optimal linear estimation of the data is obtained by the non-negative constraint. NMF can be easily described as follows: a non-negative matrix of all elements can be approximated with the product of the two matrix and all elements of the two matrix are non- negative, as shown in the formula (4).

$$V_{M\times N} = W_{M\times R} H_{R\times N} + \varepsilon \tag{4}$$

Where V is an M×N matrix, and W is an M×R matrix and H is an R×N matrix. R is the dimension of non-negative matrix factorization. In general, when the dimension R meets the conditions of the formula (5), the reduced dimension representation of V can be abtained. Especially, when $R=1$, the feature matrix W corresponds to all the features of the image.

$$R < \frac{MN}{M+N} \tag{5}$$

The formula (4) can be expressed as the form of vector scalar product:

$$V_j \approx \sum_{i=1}^{R} W_i \cdot H_{ij} \tag{6}$$

Where, V_j represents the j-th column vector of the V ; W_i is the i- th column vector of the W. $V=[V_1 \quad V_2 \quad \cdots \quad V_j]$, $W=[W_1 \quad W_2 \quad \cdots \quad W_i]$. As seen in Eq.6, the corresponding element in the matrix W and H can be used to approximatly express each column in the matrix V. Therefore, W is the basis matrix and H is the coefficients matrix. When W contains the essential features of the image, $V \approx WH$.

The formula (4) and (6) are the mathematical model of the NMF of the data V.

3. An Algorithm of Medical Image Fusion Based on NSST and NMF

3.1. Fusion Frame

The images to be fused are A and B, and the fused images is F. The framework diagram of the image fusion based on NSST and NMF is shown in Figure 3. As shown in Figure 3, AL and BL represent the low frequency coefficients of the images of A and B, $AH^{j,k}$ and $BH^{j,k}$ represent the k-th high frequency coefficients in the j-th layer of the images of A and B.

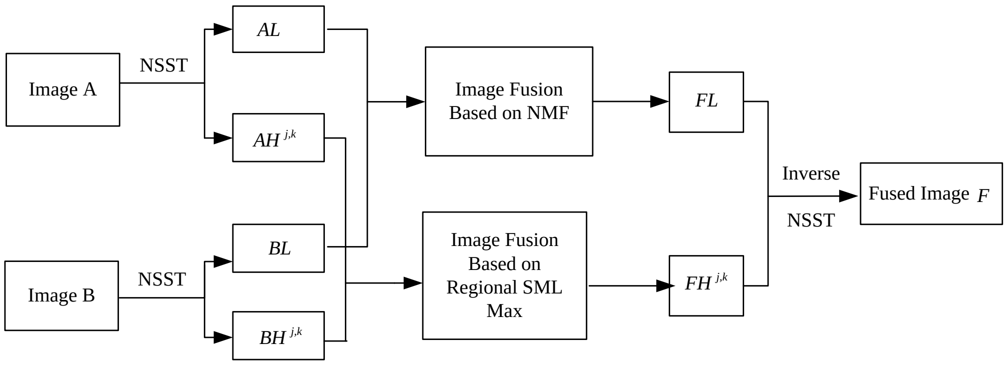

Figure 3. Schematic Diagram of Medical Image Fusion Algorithm Based on NSST

The specific steps of the medical image fusion based on NSST and NMF are as follows:

Step 1: Image A and image B should be registrated, the precision determines the effect of fusion. In this paper, A and B have been registrated completly.

Step 2: Using the NSST decomposition to achieve the low frequency $\{AL, AH^{j,k}\}$ and high frequency coefficients $\{BL, BH^{j,k}\}$ of the image A and B. In this paper, the decomposition level is set as 3, *i.e.* $j \in \{1,2,3\}$. Where, $j = 1, k = 4$; $j = 2, k = 4$; $j = 3, k = 8$.

Step 3: The low frequency coefficient FL of the fused image is obtained using NMF to select the AL and BL decomposed from Step 2;

Step 4: Using the strategy called "Regional Sum Modified-Laplacian Maximum" to fuse high-frequency coefficients $AH^{j,k}$ and $BH^{j,k}$ decomposed from Step 2 to get the $FH^{j,k}$ of the fused image F .

Step 5: The NSST inverse transform is exerted on the $\{FL, FH^{j,k}\}$ obtained from the Step 3 and Step 4 to reconstruct the final fused image F.

3.2. The Fusion Rule of the Low Frequency Coefficients

The two low frequency images AL and BL are fused using the NMF algorithm. The specific implementation steps are:

Step 1: The low frequency image AL and BL are respectively organized into column vectors in the form of VL_A and VL_B in accordance with the priority of row. The size of the image AL and BL is $M \times N$, and the size of the column vectors VL_A and VL_B is $MN \times 1$, as shown in Eq. 10.

$$VL_A = \begin{bmatrix} v_{1AL} \\ v_{2AL} \\ \cdots \\ v_{MNAL} \end{bmatrix}_{MN\times 1}, \quad VL_B = \begin{bmatrix} v_{1BL} \\ v_{2BL} \\ \cdots \\ v_{MNBL} \end{bmatrix}_{MN\times 1} \tag{10}$$

Step 2: Using the column vectors VL_A and VL_B to construct the original data matrix VL.

$$VL = [VL_A, VL_B]_{MN\times 2} = \begin{bmatrix} v_{1AL} & v_{1BL} \\ v_{2AL} & v_{2BL} \\ \cdots & \cdots \\ v_{MNAL} & v_{MNBL} \end{bmatrix}_{MN\times 2} \tag{11}$$

Step 3: Set $r = 1$, the Euclidean distance function is selected as a target function, and the iterative value of W and H is initialized, and the initial maximum number of iterations is set to 1000, and the iteration stop condition is $\varepsilon = 10^{-3}$.

Step 4: After setting the parameters, the original data matrix VL is decomposed by NMF, getting two matrices(W is the basis matrix , H is the weight coefficient matrix).

$$VL_{MN\times 2} = W_{MN\times 1} H_{1\times 2} = \begin{bmatrix} w_1 \\ w_2 \\ \cdots \\ w_{MN} \end{bmatrix} \begin{bmatrix} h_1 & h_2 \end{bmatrix} \tag{12}$$

Step 5: The matrix W can be got after certain times of iterations, and which will be used to construct the low frequency image FL.

3.3. The Fusion Rule of the High Frequency Coefficients

In a certain extent, the Sum Modified-Laplacian (SML) can properly characterize the detail information and clarity of the image. Compared with other methods, SML has a better discrimination ability and great fusion performance. In order to obtain a fusion image with better visual effect and more detail information, this paper proposes a "Regional SML Max" fusion method of high frequency sub-band coefficient.

The high frequency sub-band coefficients are represented with the $PH^{j,k}(r,c)$, where, j , k indicate the scale and the direction of the location (r,c) respectively. The Sum-modified-Laplacian $SML_{PH}^{j,k}(r,c)$ is defined as follows:

$$ML_{PH}^{j,k}(r,c) = \left|L_x * PH^{j,k}(r,c)\right| + \left|L_y * PH^{j,k}(r,c)\right|, P = A, B \tag{13}$$

Where, L_x and L_y are the two-order difference operator in x direction and y direction.

$$L_x = \begin{bmatrix} -1 & 2 & -1 \end{bmatrix}, \; L_y = L_x^T = \begin{bmatrix} -1 & 2 & -1 \end{bmatrix}^T \tag{14}$$

$$SML_{PH}^{j,k}(r,c) = \sum_{n=-(N-1)/2}^{(N-1)/2} \sum_{m=-(M-1)/2}^{(M-1)/2} \left[ML_{PH}^{j,k}(r+m, c+n)\right]^2, P = A, B \tag{15}$$

Where, $M \times N$ represents the size of the local area with (r,c) as the center, and the size is set as 3×3.

The high frequency sub-band coefficients $FH^{j,k}$ after fusion is given by:

$$FH^{j,k}(r,c) = \begin{cases} AH^{j,k}(r,c), & SML_{AH}^{j,k}(r,c) \ge SML_{BH}^{j,k}(r,c) \\ BH^{j,k}(r,c), & SML_{AH}^{j,k}(r,c) < SML_{BH}^{j,k}(r,c) \end{cases} \tag{16}$$

4. Experimental Results and Discussion

The 2 sets of medical images shown in Figure 4 are chosen to verify the effectiveness and correctness of the proposed algorithm. The medical images are all from the "The Visible Human Project" data library, which is sponsored by U.S. National Library of Medicine. The experimental platform is the Matlab2011 (a), and the configuration of the host computer: Intel (R) CPU processor, clocked at 3.4GHz, 8GB memory.

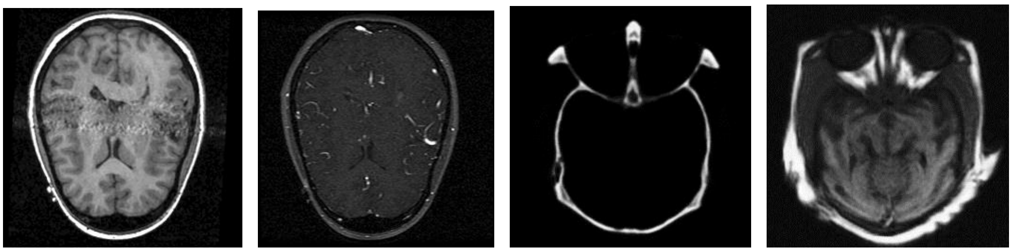

(a) CT-Brain (b) MRI-Brain (c) CT-Head (d) MRI-Head

Figure 4. Medical Source Images

The other 2 algorithms, including NSST-based algorithm and NMF-based algorithm are used to compare with proposed approach. In the NSST-based algorithm, NSST is set to 3 layers scale decomposition, and in accordance with the resolution layer from "rough" to "fine ", the number of the shear directions is set to $\{4,8,8\}$; In NMF-based algorithm, the number of iterations is set to 1000. Because the random values of the basis matrix W and the weight coefficient matrix H will have a great effect on the final fusion results, this paper chooses the fused image with the maximum information entropy from the three simulations as a final simulation result. In the algorithm proposed in this paper, the setting of NSST is consistent with NSST-based algorithm, NMF's setting consistent with NMF-based algorithm. For all the algorithms, the fusion rule adopts the fusion method proposed in this paper. The fusion results are shown in Figure 5 and Figure 6.

In this paper, to make a comprehensive evaluation for the quality of the images fused by a variety of methods, five parameters are adopted, such as Entropy (E), Average gradient (AG), Standard deviation (SD), edge information retention capacity ($Q^{AB/F}$) and spatial frequency (SF). Compared with other algorithms, the algorithm proposed in this paper can get better visual effect. The results are shown in Table 1 and Table 2.

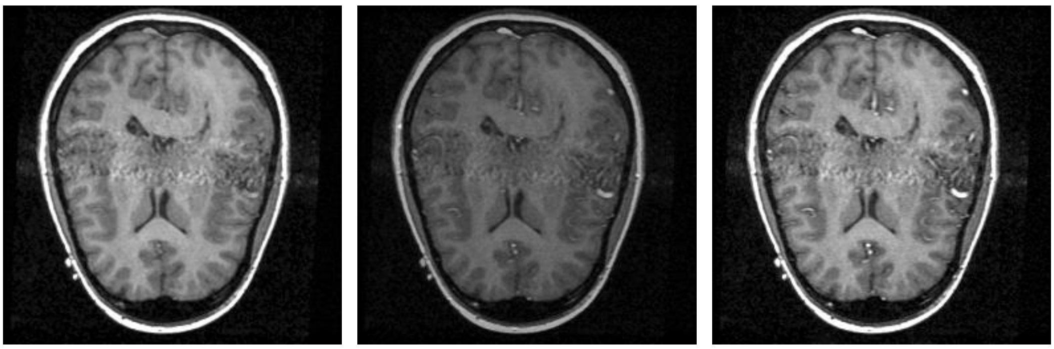

(a) NMF (b) NSST (c) NSST+NMF

Figure 5. Fusion Results on "Brain" Image

Table 1. Comparison of Medical "Brain" Image

	E	AG	$Q^{AB/F}$	SF	SD
NMF	6.4351	7.0798	0.4690	16.3293	70.5499

NSST	6.8579	11.4589	0.5544	26.6348	70.3709
NSST+NMF	7.1071	14.9245	0.6118	29.3861	44.6337

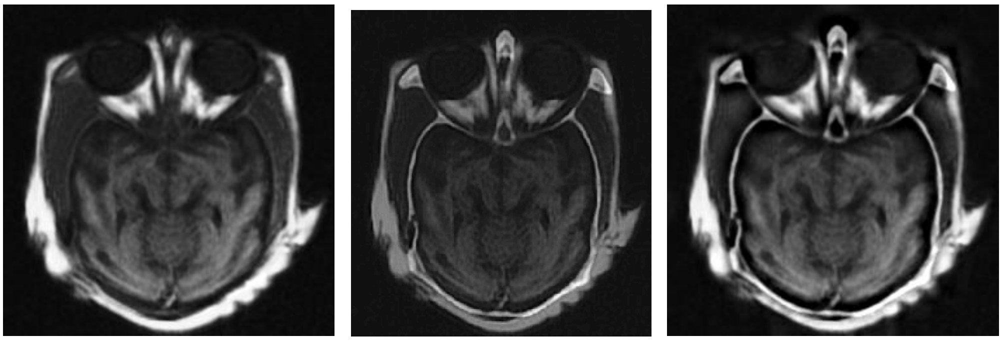

(a) NMF (b) NSST (c) NSST+NMF

Figure 6. Fusion Results on “Head” Image

Table 2. Comparison of Medical “Head” Image

	E	AG	$Q^{AB/F}$	SF	SD
NMF	6.6561	5.7651	0.6372	14.7564	59.3099
NSST	6.6585	7.4474	0.6421	17.5293	57.1152
NSST+NMF	7.1559	8.1665	0.7106	21.7660	45.2292

From Figure 6 we can see that the three kinds of fusion algorithms can achieve effective fusion for the CT and MRI images. The algorithm can not only highlight the profile information of the target, but also can reflect the details. Enlarging the fusion images, it can be seen that the hierarchy and the resolution is higher in Figure6 (c). Compared with other algorithms, the algorithm proposed in this paper can get better visual effect. From Table 1 and Table 2, we can see that in the aspect of the objective parameter evaluation, the method proposed in this paper is better than the other fusion methods in the comparison of SD, E, AG, $Q^{AB/F}$ and SF.

5. Conclusion

When the source images are decomposed with NSST, the transform coefficients have great redundancy. NSST is essentially a redundant transform, which cannot be used alone to remove redundant information effectively. In order to reduce the redundant information, an image fusion algorithm based on NSST and NMF is proposed. The algorithm combining NSST and NMF can not only effectively remove the redundant information, and get a comprehensive extraction of all the characteristics of multi-source image, but also can fully extract the information of the direction details of the image. Experiments show that, the proposed algorithm can achieve effective fusion of the medical images, and the visual effect of the fused image is better, and the structure information of the source images can be more transfer to the fusion images. The presented algorithm is superior to other fusion algorithms from the objective parameters.

Acknowledgements

The authors would like to thank for the developers of the shearlet toolbox. This work is supported by Jilin Province Education Department (No. 20140529) and the "Chunhui" Project of the National Ministry of Education (No. Z2014138).

References

[1] K. Guo, D. Labate and W. Q. Lim, "Wavelets with composite dilations and their MRA properties", Applied and Computational Harmonic Analysis, vol.20, no.2, **(2006)**, pp. 202-236.
[2] W. Q. Lim. "The Discrete Shearlet Transform: A New Directional Image Representation and Compactly Supported Shearlet Frames", IEEE Transactions on Image Processing, vol.19, no.5, **(2010)**, pp. 1166-1180.
[3] T.-T. Bai, C.-X. Deng and Y. Geng, "Image Edge Detection Based on Wavelet Transform and Canny Operator", Journal of Harbin University of Science and Technology, vol. 15, no.1, **(2010)**, pp. 44-48.
[4] D. D. Lee and H. S. Seung, "Learning the Parts of Objects by Non-Negative Matrix Factorization", Nature, vol. 401, no.21, **(1999)**, pp. 788-791.
[5] D. D. Lee and H. S. S., "Algorithms for Non-negative Matrix Factorization", Proc of Advances in Neural and Information Processing Systems, **(2000)**, pp. 556-562.
[6] L.-R. Hu, "Method for Non-negative Matrix Factorization and Its Application in Ballot Image Recognition", Graduate of Anhui University, Ph.D. Thesis, **(2013)**.
[7] A. Frigyesi and M. Hoglund, "Non-negative matrix factorization for the analysis of complex gene expression data: identification of clinically relevant tumor subtypes", Cancer Informatics, vol. 6, **(2008)**, pp. 275-292.
[8] M. Ouhsain and A. B. Hamza, "Image watermarking scheme us-ing nonnegative matrix factorization and wavelet transform", Expert Systems with Applications, vol. 36, no.2, **(2009)**, pp. 2123-2129.
[9] Y.-P. Zhang, W.-C. Zheng and X.-H. Zhang, "Nonnegative matrix factorization and its applications in data compression", Journal of Xi'an University of Post and Telecommunications, vol.13, no. 3, **(2008)**, pp. 58-61.
[10] A. Cichocki and R. Zdunek, "MultiIayer Nonnegative Matrix factorization using Projected Gradient A-pproaches", International Journal of Neural Systems, vol.17, no.6, **(2008)**, pp. 431-446.
[11] Y. Wu and F. Tao, "Multispectral and Panchromatic Image Fusion Based on Improved Projected Gradient NMF in NSST Domain" , Acta Optica Sinica, vol. 35, no.4, **(2015)**, pp.139-148.
[12] L.-Q. Zeng and H.-S. Tong, "Application of Non-negative Matrix Factorization and Curvelet to Remote Sensing Image Fusion", Journal of East China Institute of Technology(Natural Science), vol.36, no.4, **(2013)**, pp.415-418.
[13] K. Guo and D. Labate, "Optimally Sparse Multidimensional Representation using Shearlets", SIAM JMathl Anal, vol. 39, **(2007)**, pp. 298-318.
[14] G. Easley, D. Labate and W. Lim, "Sparse Directional Image Representation using the Discrete Sheralet Transform", Appl Comput Harmon Anal, vol. 25, no. 1, **(2008)**, pp. 25-46.
[15] L. Wang, B. Li and L. F. Tian, "Medical Image Fusion Based on Shift-Invariant Shearlet Transformation", Journal of South China University of Technology (Natural Science Edition), vol. 39, no.12, **(2011)**, pp.13-19.
[16] Y. H. Gao, G. Q. Chen and Y. Y. Liu, "Adaptive image fusion based on image quality assessment parameter in NSST domain", Journal of Jilin University (Engineering and Technology Edition), vol. 43, no.1, **(2014)**, pp. 225-234.

